Electrocatalysis

International Edition: DOI: 10.1002/anie.201701984
German Edition: DOI: 10.1002/ange.201701984

Chemical Recognition of Active Oxygen Species on the Surface of Oxygen Evolution Reaction Electrocatalysts

*Chunzhen Yang, Olivier Fontaine, Jean-Marie Tarascon, and Alexis Grimaud**

Abstract: *Owing to the transient nature of the intermediates formed during the oxygen evolution reaction (OER) on the surface of transition metal oxides, their nature remains largely elusive by the means of simple techniques. The use of chemical probes is proposed, which, owing to their specific affinities towards different oxygen species, unravel the role played by these species on the OER mechanism. For that, tetraalkylammonium (TAA) cations, previously known for their surfactant properties, are introduced, which interact with the active oxygen sites and modify the hydrogen bond network on the surface of OER catalysts. Combining chemical probes with isotopic and pH-dependent measurements, it is further demonstrated that the introduction of iron into amorphous Ni oxyhydroxide films used as model catalysts deeply modifies the proton exchange properties, and therefore the OER mechanism and activity.*

Water splitting has been envisioned for decades as a promising strategy to produce clean and renewable hydrogen for energy storage. However, this process is largely hampered by the slow kinetics associated with the oxygen evolution reaction (OER), $2H_2O \rightarrow O_2 + 4H^+ + 4\,e^-$. Therefore, numerous studies have been conducted to understand and control this reaction.[1–3] While progress was made on the design of electrocatalysts for the OER, these studies point to the correlation between the activity and the stability for OER catalysts. The surface of the most active oxides reconstructs during OER, resulting in amorphous oxyhydroxide structure, which consists of clusters of edge-shared octahedra.[4,5]

One factor distinguishing molecular catalysts from solid catalysts is that, aside from their homogeneous nature, the electrochemically formed high-valence metal–oxo species can form an O–O bond by either an acid–base reaction with water or via the direct coupling of two neighboring oxo species.[2,6,7] In contrast, for heterogeneous catalysts, the OER is believed to proceed via four consecutive proton-coupled electron transfer (PCET) steps, with the metallic center serving as active site (Supporting Information, Figure S1).[8] Nevertheless, the recent findings that surface oxygen can also act as active site on the surface of OER electrocatalysts bolsters the idea that a mechanism enlisting continuous bond-breaking and -formation can be at play on the surface of some catalysts,[9–11] eventually leading to their instability under oxidative conditions.[12–14] Interestingly, amorphous structures lie at the frontier between heterogeneous and homogeneous catalysts but the exact nature of the active site as well as their interaction with the adsorbed water molecules remain unclear. Moreover, even though agreement has been largely reached recognizing that deprotonation is key for the formation of the so-called active oxygen species,[15–17] their exact nature and reactivity remains elusive, owing to their transient nature and the lack of proper characterization techniques.[18]

Nickel oxyhydroxide is the most ubiquitous OER catalyst in alkaline media and demonstrates exceptionally large activity. A recent report by the Boettcher group demonstrated that iron contamination is at the origin of its large OER activity.[19] Subsequent studies have shown that iron serves multiple purposes for Ni(Fe)OOH catalysts:[20] 1) it adopts a different local environment with unusually short Fe–O bond distance as shown by operando X-ray absorption spectroscopy (XAS);[21] 2) it modifies the redox activity of nickel;[17] and 3) it improves the electronic conductivity of the film.[22] We demonstrate herein that introducing iron also induces the formation of active oxygen species, which demonstrate specific interactions with interfacial water. For that, we alleviate the difficulty for studying transient active species by introducing a new chemical approach. This approach is inspired by previous reports discussing the effect of hydration shell for electrocatalytic reactions[23,24] and makes use of cations showing specific interactions with active oxygen species. More specifically, we introduce tetraalkylammonium cation (TAA^+) as a chemical probe in solution and demonstrate its specific interaction with oxygen species formed upon deprotonation. Comparing the OER

[*] Dr. C. Yang, Prof. J.-M. Tarascon, Dr. A. Grimaud
Chimie du Solide et de l'Energie, Collège de France, UMR 8260
75231 Paris Cedex 05 (France)
E-mail: alexis.grimaud@college-de-france.fr
Prof. O. Fontaine
Institut Charles Gerhardt Montpellier
Université Montpellier, UMR 5253
Place Eugène Bataillon, 34095 Montpellier (France)
Prof. O. Fontaine, Prof. J.-M. Tarascon, Dr. A. Grimaud
Réseau sur le Stockage Electrochimique de l'Energie (RS2E)
CNRS FR3459
33 rue Saint Leu, 80039 Amiens Cedex (France)
Prof. J.-M. Tarascon
Department of Chemistry, UPMC
4 Place Jussieu, 75005 Paris (France)
and
ALISTORE-European Research Institute, FR CNRS 3104
80039 Amiens (France)

Supporting information for this article can be found under: https://doi.org/10.1002/anie.201701984.

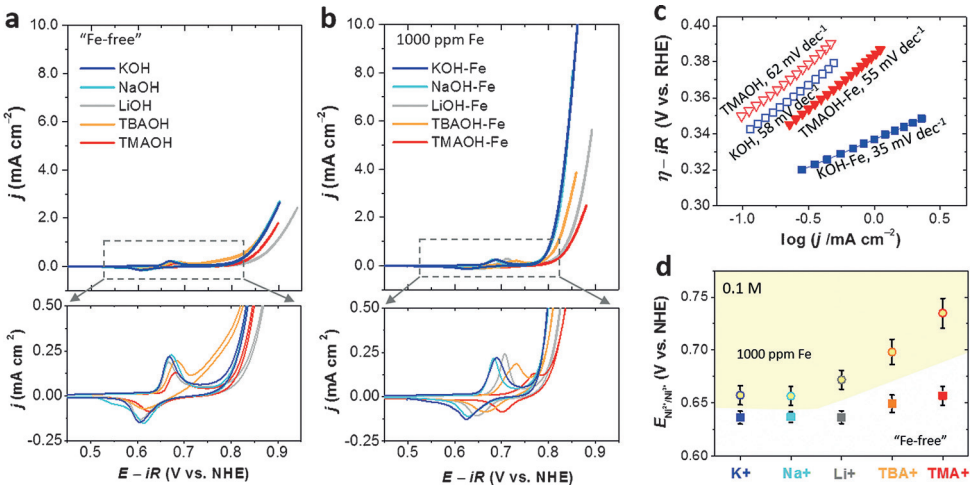

Figure 1. Cyclic voltammograms for NiOOH films when using a) 0.1 M MOH purified solution and b) solutions containing 1000 ppm Fe. c) Tafel plots for the OER activities measured with KOH and TMAOH purified and Fe-containing solutions. d) Redox potential of $Ni(OH)_2$/NiOOH in 0.1 M MOH solutions.

activities of Fe-free and Fe-containing amorphous films, we demonstrate that these interactions only occur for Fe-containing Ni(Fe)OOH catalysts. By blocking these active surface oxygens with adsorbed TAA^+ cations, we reveal the interactions occurring at the catalyst–water interface, where modifying the structure of the interfacial water and the proton diffusion properties lead to drastic modifications of the OER mechanism and activity.

The oxidation behavior of the electrodeposited nickel oxyhydroxide films was studied by cyclic voltammetry in Fe-free 0.1M MOH solution, with M being Li^+, Na^+, K^+, TBA^+, and TMA^+ (Figure 1a). No modification of the Ni^{II} to Ni^{III} oxidation potential is observed for Li^+, Na^+, and K^+, while a moderate shift towards greater potential is observed for TBA^+ and TMA^+. For Fe-containing films, the Ni^{3+}/Ni^{2+} redox peak is largely influenced by the nature of the cation, and a shift towards greater potential as large as 78 mV was measured between K^+ and TMA^+ (Figure 1b,d). Knowing that the difference in $E_{1/2}$ measured for Li^+, Na^+, and K^+ alkaline cations is negligible (Figure 1d), the shift in standard potential cannot be simply ascribed to different solvation strengths for the different cations. The large shift of the redox potential between organic TAA^+ cations (TMA^+ and TBA^+) and alkaline cations (Li^+, Na^+, K^+) could indicate that Fe-free and Fe-containing films have different affinities towards TBA^+ and TMA^+ cations, from weak (Fe-free) to strong (Fe-containing).

In situ UV/Vis spectroscopy was then employed to further visualize the interaction between the amorphous films and TMA^+ cations. Similar electrochromic behaviors were found for purified KOH and TMAOH as well as for Fe-containing KOH solutions, with a clear decrease of the transmission correlated to the oxidation of Ni^{2+} to Ni^{3+} and the deprotonation of the film (Supporting Information, Figures S6, S7). However, while the transmission loss reaches 10% for these solutions, this value is lower when measured in Fe-containing TMAOH solution. This difference further reinforces that the Fe-containing films specifically interact with TMA^+ cations during the deprotonation/oxidation step. Looking in greater details to the Ni^{2+}/Ni^{3+} redox waves, the pure NiOOH films show, independently of the cation, a potential–pH dependence value close to −60 mV/pH indicating a ratio proton to electron exchange close to unity. For the Fe-containing films, the potential–pH dependence becomes close to −90 mV/pH for pH > 12.5. This value, characteristic of a super-Nernstian potential–pH shift corresponding to the exchange of 2 electrons and 3 protons (ratio of H^+/e^- involved equals to 1.5),[17,25] indicate a different deprotonation mechanism for Fe-containing film. Hence, depending on the deprotonation process, different oxygen species are formed on the surface of the films that show, or not, specific interaction with TMA^+ cation, as visualize by Raman spectroscopy (Supporting Information, Figure S8). This conclusion is in agreement with previous spectroscopic evidences showing the generation of negatively charged sites for Fe-containing films.[18]

Now turning to the OER activity, it is found to be nearly identical for pure NiOOH when using K^+ and TMA^+ (Figure 1c). The Tafel slope is also found to be identical and equal to circa 60 mV/decade, indicating a one-electron transfer occurring before the chemical turnover-limiting step (TLS). In contrast, the OER activity for Ni(Fe)OOH films decreases between alkaline cations (K^+ and Na^+) and TMA^+ (Figure 1c; Supporting Information, Figure S9). Moreover, a change in the Tafel slope from 35 mV/decade to 55 mV/decade is observed from alkaline cations (Na^+ and K^+) to TMA^+ cations (Figure 1c; Supporting Information, Figure S9). This observation confirms that TMA^+ can selectively modify the OER mechanism depending on its interaction with the film. Furthermore, the pH dependence for the OER activity of the Ni(Fe)OOH films was studied for TMA^+ and compared with the non-interacting K^+ cation (Supporting Information, Figure S10). For a pH value above about 12, the OER activity as well as the Tafel slopes remain constant for both cations (Tafel slopes of approx. 30 mV/decade for K^+ and approx. 60 mV/decade for TMA^+). Moreover, above pH 12, $(\partial E/\partial \mathrm{pH})i = 0$ giving a rate order for H^+ of 0 on the RHE scale, which would indicate a proton-coupled electron transfer (PCET)[26] independent of the nature of the cation. Below this pH value, the OER activity decreases and the Tafel slope is found to increase up to a value close to 90 mV/decade for TMA^+ and 60 mV/decade for K^+, indicating chemical limitations related to the deprotonation of surface oxygen and/or the proton diffusion, as recently discussed for buffered neutral solution.[27]

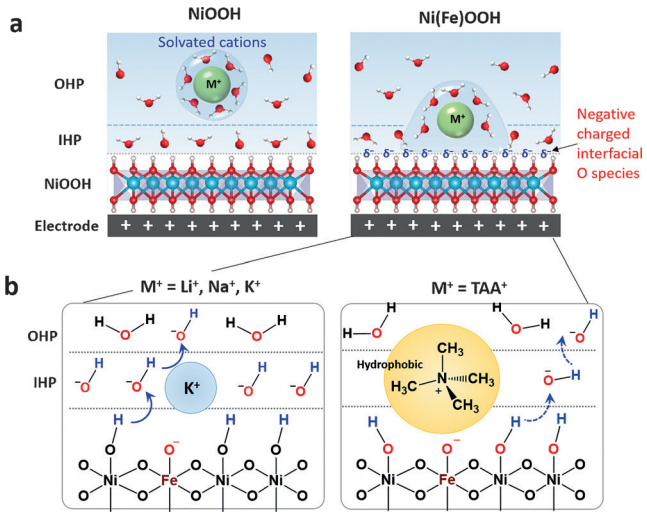

Figure 2. a) The cation interaction with active oxygen species on the surface of pure NiOOH and Fe-containing Ni(Fe)OOH film catalyst, and b) interfacial proton transfer from solid catalyst to inner Helmholtz plane (IHP) further to outer Helmholtz plane (OHP) being modified by alkaline cations (bottom left) and TAA cations (bottom right) absorption on Ni(Fe)OOH film catalyst.

To obtain further information on the OER mechanism and the role of hydrogen bonding network (Figure 2), measurements were then carried out in H_2O and D_2O solutions. For Fe-free films, switching from proton to deuterium does not modify the OER activity (Figure 3). However, for Fe-containing films, the use of deuterated water significantly decreases the OER activity in KOH solution. Not only the OER activity decreases, but also the Tafel slope increases when using deuterated water. Bearing in mind that a PCET mechanism is presumably at play independently of the use of TMA^+, the isotopic effect indicates that hydrogen bonds network must be influencing the OER kinetics by modifying either the number of active sites or the interactions of intermediates with adsorbed water. Expressing the OER current density as $j = nFK\theta_{act}e^{-\frac{\Delta G_f}{RT}}$, with θ_{act} being the concentration of active sites and ΔG_f the enthalpy of formation of the intermediate governing the rate of the reaction, the change in Tafel slope observed for Ni(Fe)OOH films when changing from H_2O to D_2O suggest a difference in the enthalpy of formation of the intermediate that governs the reaction rate. We therefore hypothesize that introducing deuterated water modifies the $*O\cdots HO^-$ interactions between active oxygen species and OH^- and eventually the enthalpy of formation of the intermediate that governs the reaction rate (presumably the formation of O–O bond).

In light of these results, we propose that the specific interaction of TMA^+ and active oxygen species displaces this equilibrium by stabilizing the active oxygen species and therefore controls the rate of the reaction. These results revealed the critical role played by the interfacial interactions on the OER kinetics.

Aside from modifying the hydrogen bonding network, cations also possess different enthalpy of hydration (Supporting Information, Table S1). Therefore, to discriminate the effects induced by specific interactions from effects induced by the modification of the solvation strength, we employed (2,2,6,6-tetramethylpiperidin-1-yl)oxyl (TEMPO) as a soluble molecular probe (Figure 4; Supporting Information, Figure S11). We first demonstrate the instability of the oxidized

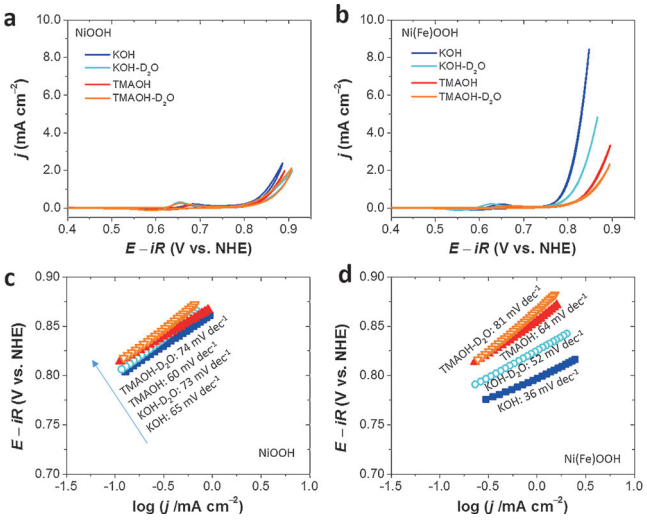

Figure 3. OER on a) pure NiOOH and b) Ni(Fe)OOH film catalyst in 0.1 M KOH and TMAOH dissolved in H_2O or D_2O (99%). c),d) Tafel slopes derived from CV curves in (a) and (b), respectively. Noted that TMAOH and KOH with the same concentration give negligible difference on pH values.[28] Both 0.1 M KOH and TMAOH dissolved in high-purified H_2O show a pH of about 13.0, whereas in D_2O are about 13.3, as previously discussed.

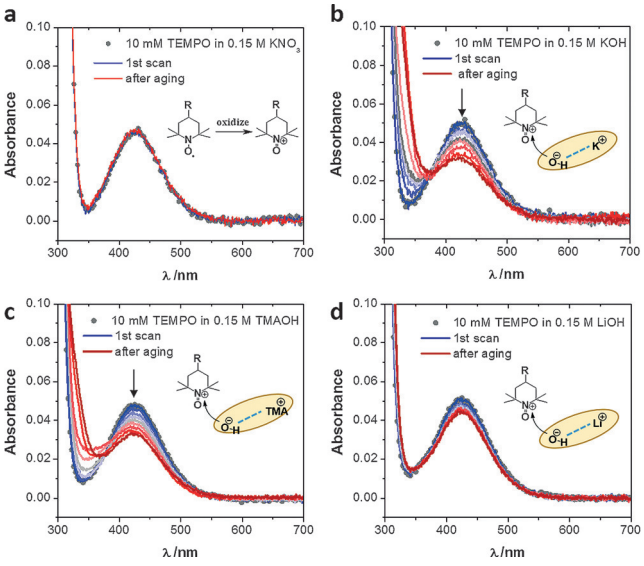

Figure 4. UV/Vis studies of TEMPO disproportionation and reactivity with water in 0.15 M aqueous solutions of a) KNO_3, b) KOH, c) TMAOH and d) LiOH. The reactivity towards $TEMPO^+$ reflects the ion paring strength between hydroxide anions and alkaline/TAA cations. The 10 mM TEMPO solution was firstly charged at 0.8 V vs. Ag/AgCl for 40 mins, and then left aging for 10 h. During the aging period, UV/Vis spectroscopy was carried out every 30 mins.

form of TEMPO in alkaline solution by using UV/Vis, as well as the effect of cation on this instability. For that, we followed the decrease of the UV absorbance at approximatively 430 nm corresponding to the oxidized form of TEMPO (Figure 4). More specifically, the drop of absorbance was measured to be dependent on the cation, with TMA^+ and K^+ showing a fast drop of the signal corresponding to a decay of the concentration in $TEMPO^+$ (Figure 4a and b), while the decrease was found much slower for Li^+ (Figure 4c). We estimated the kinetic rate constant to be rather similar for K^+ and TMA^+ ($k = 0.18\ s^{-1}$ and $0.12\ s^{-1}$, respectively), and slower when using Li^+ ($k = 0.02\ s^{-1}$; Supporting Information, Figure S11). This indicates that the kinetics associated with the nucleophilic attack of water on oxidized electrophilic species is decreased when increasing the solvation strength from K^+ (or TMA^+) to Li^+ (Supporting Information, Table S1). Bearing in mind that the OER kinetics measured for Fe-free NiOOH films was found identical in KOH and TMAOH (Figure 1c), modification of the hydration strength can be ruled out as the origin for the modifications of the OER activity of Fe-containing films when introducing TMA^+.

In conclusion, we demonstrate that due to the specific interactions of TMA^+ cations with active oxygen species formed upon deprotonation,[29] its presence on the surface of Fe-containing films disrupts the hydrogen bonds network with interfacial water. Hence, we experimentally reveal that the OER mechanism and activity is sensitive on these specific interactions (Figure 1c). We further postulate that the O–O bond formation on the surface of amorphous film, which is often considered as rate determining step for the OER, is sensitive to the distribution and the energy of the active oxygen species formed after a deprotonation step and that act as active sites. This conclusion is further supported by the H/D isotopic effect (Figure 4), which suggests that the introduction of iron in the Ni oxyhydroxide films induces a change in the interaction between active oxygen species and OH^- groups in the inner Helmholtz plane. This effect is complementary with the modification of the electronic properties previously unraveled. Hence, these findings allow us to confirm that the large difference observed between pure NiOOH and Fe-containing Ni(Fe)OOH films is not related to the interlayer distance and an increase of active sites concentration.[22] This large increase in activity is most certainly due to the modification of the interfacial interactions which govern the reaction pathway.

While the introduction of TMA^+ cations in practice reduces the OER activity for these model catalysts, tuning the double layer structure should be seen as a blessing to tune the selectivity of other reactions such as alcohol oxidation but also oxygen reduction or CO_2 reduction by modifying the reaction landscape.

Acknowledgements

We thank M.-L. Doublet, J.-S. Fillhol, M. Saubanère, and C. Robert-Laberty for fruitful discussions. We would also like to thank Nenad Markovic for insightful comments. C.Y., J.-M.T., and A.G. acknowledge funding from the European Research Council (ERC) (FP/2014)/ERC Grant-Project 670116-ARPEMA.

Conflict of interest

The authors declare no conflict of interest.

Keywords: deprotonation · isotopic effect · nickel oxyhydroxide · oxygen evolution reaction

How to cite: *Angew. Chem. Int. Ed.* **2017**, *56*, 8652–8656
Angew. Chem. **2017**, *129*, 8778–8782

[1] W. Hong, M. Risch, K. A. Stoerzinger, A. J. L. Grimaud, J. Suntivich, Y. Shao-Horn, *Energy Environ. Sci.* **2015**, *8*, 1404–1427.
[2] H. Dau, C. Limberg, T. Reier, M. Risch, S. Roggan, P. Strasser, *ChemCatChem* **2010**, *2*, 724–761.
[3] J. Herranz, J. Durst, E. Fabbri, A. Patru, X. Cheng, A. A. Permyakova, T. J. Schmidt, *Nano Energy* **2016**, *29*, 4–28.
[4] M. Risch, A. Grimaud, K. J. May, K. A. Stoerzinger, T. J. Chen, A. N. Mansour, Y. Shao-Horn, *J. Phys. Chem. C* **2013**, *117*, 8628–8635.
[5] K. J. May, C. E. Carlton, K. A. Stoerzinger, M. Risch, J. Suntivich, Y. Lee, A. Grimaud, Y. Shao-Horn, *J. Phys. Chem. Lett.* **2012**, *3*, 3264–3270.
[6] T. A. Betley, Q. Wu, T. Van Voorhis, D. G. Nocera, *Inorg. Chem.* **2008**, *47*, 1849–1861.
[7] M. G. Mavros, T. Tsuchimochi, T. Kowalczyk, A. Mcisaac, L. Wang, T. Van Voorhis, *Inorg. Chem.* **2014**, *53*, 6386–6397.
[8] I. C. Man, H.-Y. Su, F. Calle-Vallejo, H. A. Hansen, J. I. Martínez, N. G. Inoglu, J. Kitchin, T. F. Jaramillo, J. K. Nørskov, J. Rossmeisl, *ChemCatChem* **2011**, *3*, 1159–1165.
[9] A. Grimaud, W. T. Hong, Y. Shao-Horn, J.-M. Tarascon, *Nat. Mater.* **2016**, *15*, 121–126.
[10] A. Grimaud, O. Diaz-Morales, B. Han, W. T. Hong, Y.-L. Lee, L. Giordano, K. A. Stoerzinger, M. T. M. Koper, Y. Shao-Horn, *Nat. Chem.* **2017**, *9*, 457-465.
[11] J. T. Mefford, X. Rong, A. M. Abakumov, W. G. Hardin, S. Dai, A. M. Kolpak, K. P. Johnston, K. J. Stevenson, *Nat. Commun.* **2016**, *7*, 11053.
[12] A. Grimaud, A. Demortiere, M. Saubanere, W. Dachraoui, M. Duchamp, M. Doublet, J. Tarascon, *Nat. Energy* **2016**, *2*, 16189.
[13] T. Binninger, R. Mohamed, K. Waltar, E. Fabbri, P. Levecque, R. Kötz, T. J. Schmidt, *Sci. Rep.* **2015**, *5*, 12167.
[14] X. Rong, J. Parolin, A. M. Kolpak, *ACS Catal.* **2016**, *6*, 1153–1158.
[15] D. K. Bediako, Y. Surendranath, D. G. Nocera, *J. Am. Chem. Soc.* **2013**, *135*, 3662–3674.
[16] O. Diaz-morales, D. Ferrus-Suspedra, M. T. M. Koper, *Chem. Sci.* **2016**, *7*, 2639–2645.
[17] M. Görlin, J. Ferreira de Araújo, H. Schmies, D. Bernsmeier, S. Dresp, M. Gliech, Z. Jusys, P. Chernev, R. Kraehnert, H. Dau, et al., *J. Am. Chem. Soc.* **2017**, *139*, 2070–2082.
[18] B. J. Trzesniewski, O. Diaz-Morales, D. A. Vermaas, A. Longo, W. Bras, M. T. M. Koper, W. A. Smith, *J. Am. Chem. Soc.* **2015**, *137*, 15112–15121.
[19] L. Trotochaud, J. K. Ranney, K. N. Williams, S. W. Boettcher, *J. Am. Chem. Soc.* **2012**, *134*, 17253–17261.
[20] F. Dionigi, P. Strasser, *Adv. Energy Mater.* **2016**, *6*, 1600621.
[21] D. Friebel, M. W. Louie, M. Bajdich, K. E. Sanwald, Y. Cai, A. M. Wise, M. J. Cheng, D. Sokaras, T. C. Weng, R. Alonso-Mori, et al., *J. Am. Chem. Soc.* **2015**, *137*, 1305–1313.
[22] L. Trotochaud, S. L. Young, J. K. Ranney, S. W. Boettcher, *J. Am. Chem. Soc.* **2014**, *136*, 6744–6753.

[23] V. R. Stamenkovic, D. Strmcnik, P. P. Lopes, N. M. Markovic, *Nat. Mater.* **2016**, *16*, 57 – 69.
[24] A. Fortunelli, W. A. Goddard III, L. Sementa, G. Barcaro, *Nanoscale* **2015**, *7*, 4514 – 4521.
[25] R. L. Doyle, I. J. Godwin, M. P. Brandon, M. E. G. Lyons, *Phys. Chem. Chem. Phys.* **2013**, *15*, 13737 – 13783.
[26] L. Giordano, B. Han, M. Risch, W. T. Hong, R. R. Rao, K. A. Stoerzinger, Y. Shao-Horn, *Catal. Today* **2016**, *262*, 2 – 10.
[27] D. K. Bediako, C. Costentin, E. C. Jones, D. G. Nocera, J.-M. Savéant, *J. Am. Chem. Soc.* **2013**, *135*, 10492 – 10502.
[28] P. K. Glasoe, F. A. Long, *J. Phys. Chem.* **1960**, *64*, 188 – 190.
[29] H. B. Srmemann, G. Braun, W. Brijoux, R. Brinkmann, A. S. Tilling, K. Seevogel, K. Siepen, *J. Organomet. Chem.* **1996**, *520*, 143 – 162.

Manuscript received: February 23, 2017
Accepted manuscript online: May 31, 2017
Version of record online: June 21, 2017

